EQUILIBRIUM EVAPORATION BENEATH A GROWING CONVECTIVE BOUNDARY LAYER

ALISTAIR D. CULF

Institute of Hydrology, Wallingford, Oxon OX10 8BB, UK

(Received in final form 23 November, 1993)

Abstract. Expressions for the equilibrium surface Bowen ratio (β_s) and equilibrium evaporation are derived for a growing convective boundary layer (CBL) in terms of the Bowen ratio at the top of the mixed layer (β_i) and the entrainment parameter A_R. If A_R is put equal to zero, the solution for β_s becomes that previously obtained for the zero entrainment or 'closed box' model. The Priestley-Taylor parameter α is also calculated and plotted in terms of A_R and β_i. Realistic combinations of the atmospheric parameters give values of α in the range 1.1 to 1.4.

1. Introduction

As an air mass moves over a region of uniform wetness, with a constant surface resistance to evaporation, the specific humidity deficit at the surface tends towards an equilibrium value (McNaughton and Jarvis, 1983; McNaughton, 1976). The Bowen ratio at the surface, β_s, then tends towards

$$\beta_s = \frac{1}{\epsilon} \tag{1}$$

where $\epsilon = s\lambda/c_p$, s is the slope of the saturated humidity curve, λ is the latent heat of vaporisation of water and c_p is the specific heat capacity of air at constant pressure. Combining Equation (1) with the surface energy balance

$$H_s + \lambda E_s = R_n - G \tag{2}$$

where H_s is the sensible heat flux, E_s is the water vapour flux, R_n is the net radiation and G is the soil heat flux, leads to the following expression for the evaporation

$$\lambda E_s = \frac{\epsilon}{(1+\epsilon)}(R_n - G). \tag{3}$$

McNaughton (1976) describes this as the quasi-equilibrium evaporation ('quasi' since the slope of the saturation humidity curve is not a constant), but it is often simply described as the equilibrium evaporation. The discrepancy between Equation (3) and the Priestley-Taylor (1972) equation

$$\lambda E = \alpha \frac{\epsilon}{(1+\epsilon)}(R_n - G) \tag{4}$$

Boundary-Layer Meteorology **70**: 37–49, 1994.

where α is a constant, has been the cause of much debate. Priestley and Taylor (1972) found α to vary between 1.08 and 1.34 and decided that the best estimate of α was 1.26, this being the overall mean of values obtained over land, lake and ocean. In a recent review of values of α obtained from several experiments, Pereira and Villa Nova (1992) report values ranging from 1.05 – 1.66. Equation (4) has mostly been tested on a daily basis; on an hourly scale, significant variations in α are found to occur. In some cases, reviewed by Pereira and Villa Nova (1992), α had a U-shaped variation with a minimum around noon, whilst in others, the value of α increased continuously throughout the day. Although there are many examples in the literature which seem to validate the use of Equation (4) with $\alpha \approx 1.26$ to estimate evaporation under potential conditions, at least on a daily basis, Monteith (1981) urges caution. He makes the point that there may well be many datasets which do not fit the relationship, but which, being regarded as negative results, have remained unpublished. Shuttleworth and Calder (1979) object strongly to the fact that the Priestley-Taylor equation takes no account of either the aerodynamic and physiological behaviour of the surface or of the precipitation input. They present long-term measurements of evaporation from coniferous forest which show α ranging from 0.62 to 9.69.

Despite these objections to the general and indiscriminate application of the Priestley–Taylor equation, it is a matter of interest that under potential conditions, α has often been found to be substantially higher than the value of unity predicted by theory. Monteith (1981) suggests that this discrepancy might be partially explained by the fact that the derivation of Equation (3) regards the mixed layer as a closed box to heat and vapour exchange, whereas in reality there may be entrainment of dry air through the top of the box. De Bruin (1983) and McNaughton and Spriggs (1986) subsequently developed simple numerical models of the growing atmospheric boundary layer which included various parameterisations of the entrainment process. These models were applied to the Cabauw dataset (Driedonks, 1981) and values of α ranging from 1 for moderately dry conditions, to 1.3 for a well watered surface were obtained. De Bruin (1983) showed that, on an hourly basis, α had some variation, having its largest values in the early morning and late afternoon, but was fairly constant during the hours around midday. In addition, the modelled evaporation had significant sensitivities to both the saturation deficit and to the stability of the air above the mixed layer. McNaughton and Spriggs (1986) concluded that it was not clear how the Priestley-Taylor equation took these effects into account and that this should be a matter for further study.

In the present paper, the physical basis of the Priestley-Taylor equation is investigated using the slightly different approach of considering the equilibrium evaporation at the surface for the case when the boundary layer is no longer a closed box to heat and water vapour transport. Formulae are derived for the equilibrium surface Bowen ratio and the equilibrium evaporation. These quantities

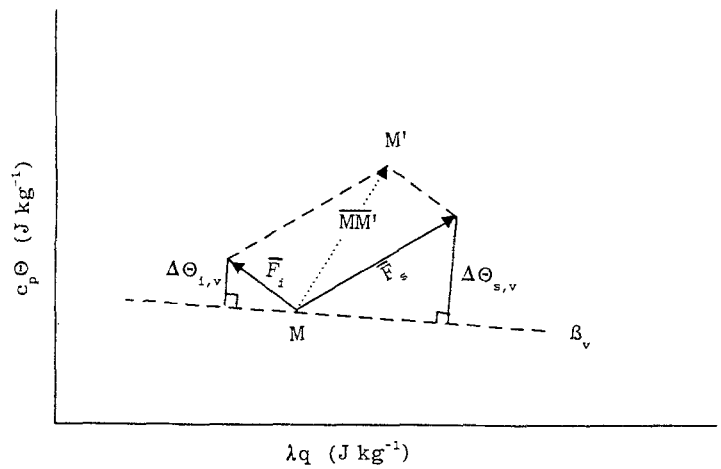

Fig. 1. Vector representation of mixed-layer growth.

are expressed in terms of the Bowen ratio at the inversion level and the rate of entrainment of air into the mixed layer from above.

2. Vector representation of the mixed layer

In a recent paper, Betts (1992) describes how simple potential temperature versus specific humidity (θ, q) diagrams can be useful for studying mixed-layer development. An example of such a (θ, q) diagram is shown in Figure 1. The initial state of the mixed layer $(c_p\theta, \lambda q)$ is M and at some time later it is M'. Betts (1992) shows how the change from M to M' can be represented on the diagram by means of vectors F_s and F_i, where F_s represents the fluxes of heat and water vapour at the surface and F_i represents the fluxes at the inversion. The gradients of these vectors on the diagram give the Bowen ratio at the surface and at the inversion, respectively.

In mixed-layer models, the flux of sensible heat at the inversion level is parameterised by means of a relationship between the virtual heat flux at the surface $H_{s,v}$ and the virtual heat flux at the inversion level $H_{i,v}$,

$$H_{i,v} = -A_R H_{S,V} \tag{5}$$

where, as throughout this work, upward directed fluxes of sensible or latent heat are defined as positive. A_R is known as the entrainment parameter. Betts (1992) shows how the vectors labelled $\Delta\theta_{i,v}$ and $\Delta\theta_{s,v}$ in Figure 1, found by projecting a perpendicular onto the dry virtual adiabat through M, are also related by the entrainment parameter,

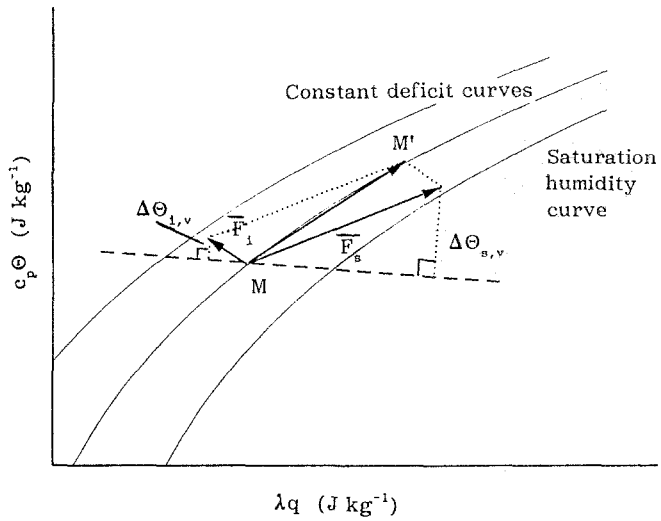

Fig. 2. Vector representation including lines of constant saturation humidity deficit.

$$\Delta\theta_{v,i} = -A_R \Delta\theta_{v,s}. \tag{6}$$

The dry virtual adiabat, labelled β_v in Figure 1, has a gradient given by $-0.608 c_p T/\lambda \approx -0.07$, where T is the temperature.

Given Equation (6), values of the Bowen ratio at the inversion, the entrainment parameter and the mixed-layer humidity and temperature, it is possible to determine the Bowen ratio at the surface from a diagram such as Figure 1. Betts (1992) uses similar diagrams to derive the surface Bowen ratio for two special cases: firstly the case when the specific humidity of the mixed layer does not change with time, and secondly when the equivalent potential temperature remains constant.

In this present work, the case considered is the case where the potential saturation humidity deficit of the mixed layer remains constant. The potential saturation deficit (e.g., McNaughton and Jarvis, 1983), given by $q^*(\theta) - q$ (where $q^*(\theta)$ is the saturation specific humidity at a potential temperature θ) is the saturation deficit that a parcel of air would attain if brought adiabatically down to the surface. It is constant throughout the mixed layer. Throughout this work, the potential temperature is referenced to the air pressure at the surface rather than the more normal 100 kPa, and therefore the potential saturation deficit and the actual saturation deficit are equal at the surface. It is possible to use Figure 1 to study this third case by adding the relationship between saturated specific humidity and temperature to the diagram. Figure 2 shows the diagram with this addition. To maintain a constant potential saturation deficit, consecutive states of the mixed layer must be parallel to this curve, i.e., M and M' must both lie on the same constant potential saturation deficit curve. Two of these curves are also plotted on Figure 2 for reference.

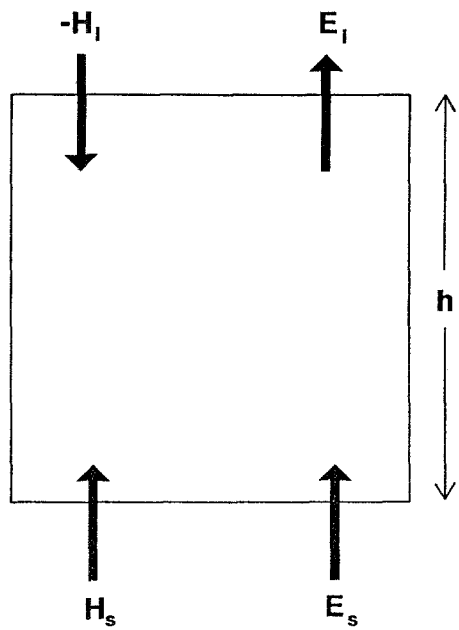

Fig. 3. The sensible heat and water vapour fluxes into and out of the box representing the convective mixed layer.

Firstly, consider the simple case of the mixed layer as a closed box. In this case the only fluxes of heat and water vapour into the box occur at the surface, and the change in state of the mixed layer from M to M' must be achieved by a single vector on Figure 2. The required vector joins the points M and M'. The surface Bowen ratio is given by the gradient of vector MM', which is simply $1/\epsilon$. This is the result obtained by McNaughton and Jarvis (1983). Now consider the more complex, but also more realistic, case when the mixed layer is no longer a closed box, but when there is a flux of warmer drier air into the mixed layer from above. In this case, the change in state of the mixed layer from M to M' must be the resultant of two vectors, one, F_s, representing the surface fluxes and the other, F_i, representing the fluxes at the inversion. It is immediately clear from Figure 2 that the Bowen ratio at the surface, i.e., the gradient of F_s, must be smaller in this case than it was for the case of the closed box. An expression for this surface Bowen ratio in terms of A_R and β_i can be derived either geometrically from a diagram such as Figure 2 or, as here, in a similar way to that used by McNaughton and Jarvis (1983) for the closed box case.

Consider the CBL as a box as shown in Figure 3. For simplicity, and following the derivation of McNaughton and Jarvis (1983), the surface layer is neglected and the potential temperature and specific humidity are assumed to be well mixed right down to the surface. The sensible heat and water vapour fluxes into and out

of the box are indicated. Note that in the text upward directed fluxes are defined as positive. Assuming conservation of energy at the floor of the box, we have, as for the closed box case, Equation 2. However, in this present case the heat and water vapour budgets of the box are given by

$$H_s - H_i = \rho c_p h \frac{\partial \theta}{\partial t} \tag{7}$$

and

$$E_s - E_i = \rho h \frac{\partial q}{\partial t} \tag{8}$$

where ρ is the density of air and h is the height of the mixed layer. Describing evaporation at the surface by the Penman-Monteith 'big leaf' model:

$$E_s = \frac{\rho[q^*(\theta) - q]}{r_c} \tag{9}$$

where r_c is the constant surface resistance to evaporation. Differentiating Equation 9 with respect to time gives

$$\frac{dE_s}{dt} = \frac{\rho\left[s\frac{\partial \theta}{\partial t} - \frac{\partial q}{\partial t}\right]}{r_c}; \tag{10}$$

so the evaporation will reach an equilibrium rate when

$$s\frac{\partial \theta}{\partial t} = \frac{\partial q}{\partial t} \tag{11}$$

i.e., referring to Figure 2, when the state of the mixed layer is moving along a constant saturation deficit curve. Consider two cases. Firstly, the strictly correct case when the virtual heat flux at the inversion level is proportional to the virtual heat flux at the surface (Equation 5). The virtual heat flux at the surface is related to the heat flux at the surface by

$$H_{s,v} = H_s - \beta_v \lambda E_s; \tag{12}$$

similarly at the inversion level

$$H_{i,v} = H_i - \beta_v \lambda E_i. \tag{13}$$

Combining Equations 5, 12 and 13 gives

$$H_i = -A_R(H_s - \beta_v \lambda E_s) + \beta_v \lambda E_i. \tag{14}$$

The latent heat flux at the inversion level is given by

$$\lambda E_i = \frac{H_i}{\beta_i}. \tag{15}$$

Combining Equations 14 and 15 gives

$$E_i = \frac{-A_R(H_s - \beta_v \lambda E_s)}{\lambda(\beta_i - \beta_v)} \tag{16}$$

and substituting for E_i in Equation 14 leads to

$$H_i = -A_R(H_s - \beta_v \lambda E_s) - \frac{\beta_v A_R(H_s - \beta_v \lambda E_s)}{(\beta_i - \beta_v)}. \tag{17}$$

The inversion-level fluxes are now expressed in terms of the surface fluxes and the Bowen ratio at the inversion level.

Equations 7 and 8 can now be written as

$$H_s + A_R(H_s - \beta_v \lambda E_s) + \frac{\beta_v A_R(H_s - \beta_v \lambda E_s)}{\beta_i - \beta_v} = \rho c_p h \frac{\partial \theta}{\partial t} \tag{18}$$

and

$$E_s + \frac{A_R(H_s - \beta_v \lambda E_s)}{\lambda(\beta_i - \beta_v)} = \rho h \frac{\partial q}{\partial t}. \tag{19}$$

Now consider the equilibrium case given by Equation 11. Using Equations 18 and 19, Equation 11 can be written as

$$\frac{\epsilon}{\lambda}\left[H_s + A_R(H_s - \beta_v \lambda E_s) + \frac{\beta_v A_R(H_s - \beta_v \lambda E_s)}{(\beta_i - \beta_v)}\right] = E_s + \frac{A_R(H_s - \beta_v \lambda E_s)}{\lambda(\beta_i - \beta_v)}. \tag{20}$$

Rearranging Equation 20 gives

$$\left[\epsilon + \epsilon A_R + \frac{\epsilon \beta_v A_R}{(\beta_i - \beta_v)} - \frac{A_R}{\beta_i - \beta_v}\right] H_s = \left[1 - \frac{A_R \beta_v}{(\beta_i - \beta_v)} + \epsilon A_R \beta_v + \frac{\epsilon \beta_v^2 A_R}{(\beta_i - \beta_v)}\right] \lambda E_s. \tag{21}$$

The Bowen ratio at the surface, β_s, is given by $H_s/\lambda E_s$, so let

$$\xi = \frac{\beta_i - \frac{1}{\epsilon}}{\beta_i - \beta_v}; \tag{22}$$

then

$$\beta_s = \frac{\frac{1}{\epsilon} + A_R \beta_v \xi}{1 + A_R \xi}. \tag{23}$$

Substituting β_s into the surface energy balance, Equation 2, leads to the following expression for the equilibrium evaporation.

$$\lambda E_s = \frac{(1 + A_R\xi)(R_n - G)}{1 + \frac{1}{\epsilon} + A_R\xi(1 + \beta_v)}. \tag{24}$$

Now consider the second case. Here it is assumed that the heat flux at the inversion level is proportional to the heat flux at the surface, rather than the relationship between the virtual heat fluxes discussed above. In this case, the fluxes at the inversion level are given by

$$H_i = -cH_s \tag{25}$$

$$\lambda E_i = \frac{-cH_s}{\beta_i}. \tag{26}$$

The effect of the simplification on Figure 2 is to rotate the dry virtual adiabats until they run perpendicular to the $c_p\,\theta$ axis and therefore have a gradient of zero. It is possible to determine the simplified expression for β_s by letting $\beta_v = 0$ in Equations 22 to 24 and replacing A_R by c, rather than repeating the derivation with Equation 25, 26 in place of Equation 17, 16, respectively. Equation 22 becomes

$$\xi' = 1 - \frac{1}{\epsilon\beta_i} \tag{27}$$

and the surface Bowen ratio is given by

$$\beta_s' = \frac{1}{\epsilon(1 + c\xi')}. \tag{28}$$

Similarly Equation 24 becomes

$$\lambda E' = \frac{1 + c\xi'(R_n - G)}{1 + \frac{1}{\epsilon} + c\xi'} \tag{29}$$

where the prime denotes that these values are calculated using the simplified entrainment relationships. Note that for the cases $A_R = 0$ and $c = 0$ (i.e., the zero entrainment cases), Equations 23 and 28 simplify to Equation 1, and Equations 24 and 29 simplify to Equation 3; the relationships previously derived for the closed box case.

3. Results and Discussion

Values of β_s were determined from Equation 23 for a range of values of A_R and β_i at three different temperatures; 10, 20 and 30 °C. The resulting values are plotted in Figure 4. Figure 4 shows that Equation 23 predicts a range of values for β_s from 0 to 0.8. However, this range can be limited by considering only the most commonly occurring combinations of the atmospheric variables β_i and A_R.

Most of the published values of the entrainment parameter A_R lie in the range 0.1 to 0.3 with $A_R = 0.2$ being the generally accepted value. However, Betts (1992) reported values of A_R close to 0.4 in a study of mixed-layer budgets for the FIFE experiment in Kansas USA, and Culf (1992) found that mixed-layer growth in the Sahel was better described by a mixed-layer model if a value $A_R = 0.5$ was used rather than 0.2. The value of β_i varies with season and according to local conditions. Betts reports a typical summer value for FIFE of -0.3, and an autumn value of -0.5. Lower values may occur when a boundary layer grows into very dry air, as is occasionally the case in the Sahel for example, and higher values occur when the mixed layer grows into the relatively unstable residual mixed layer from the previous day (Betts, 1992). Typical ranges of the two parameters are therefore -0.5 to -0.3 for β_i and 0.2 to 0.4 for A_R. The areas corresponding to these ranges of the atmospheric parameters are shaded in Figure 4. The typical ranges of the two atmospheric parameters give rise to values of β_s of 0.1 to 0.47.

The Priestley-Taylor parameter was also calculated for a range of values of A_R and β_i and for the three different temperatures. The values obtained are plotted in Figure 5.

The predicted value of α ranges from 1 to 1.8. Again the typically occurring ranges of the atmospheric parameters are plotted on the graphs. The range of α corresponding to this range of values is 1.08 to 1.46. Thus most of the range of observations of α (1.05 – 1.66) reported by Pereira and Villa Nova (1992) could be explained by various combinations of β_i, A_R and T, although it is likely that, in reality, many of these measurements were not made under equilibrium conditions.

Values of β_s and α calculated from Equations 23 and 24 for some typical values of T, A_R and β_i are given in Table I. Values of β_s' and α' calculated from the simplified Equations 28 and 29 are also shown. The simplified entrainment relationships give rise to lower values of α. The values obtained from the two methods are plotted in Figure 6 for comparison.

4. Concluding Remarks

This work shows that Equation (3) underestimates equilibrium evaporation because it is derived for the special case when there is no entrainment of dry air into the mixed layer from above. In the more general case, when entrainment is taken into account, equilibrium evaporation may be up to 1.8 times higher than

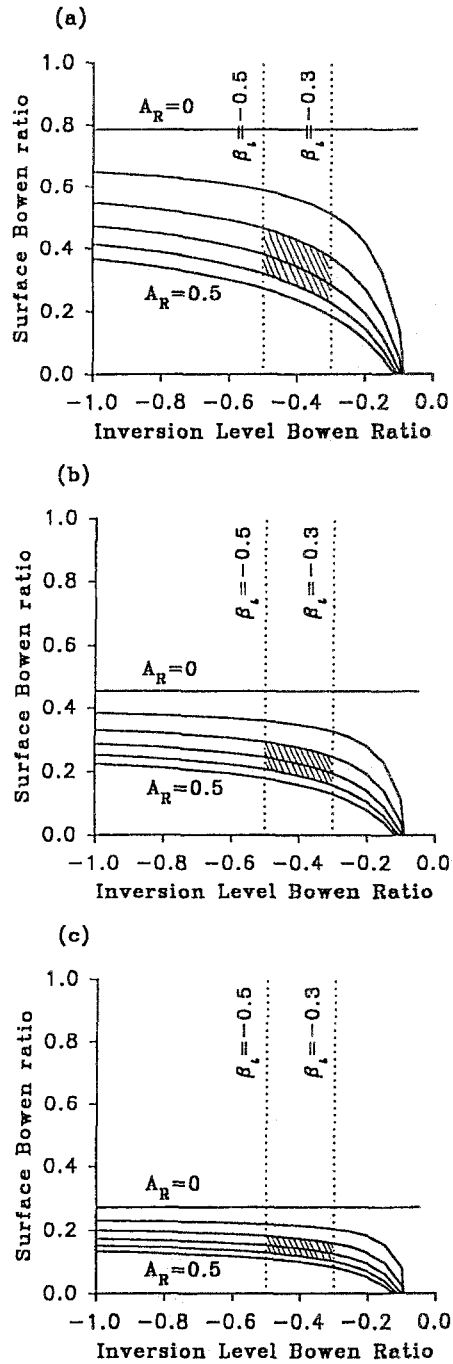

Fig. 4. Variation of the surface Bowen ratio with the entrainment coefficient and the inversion-level Bowen ratio. (a) at 10 °C, (b) at 20 °C and (c) at 30 °C.

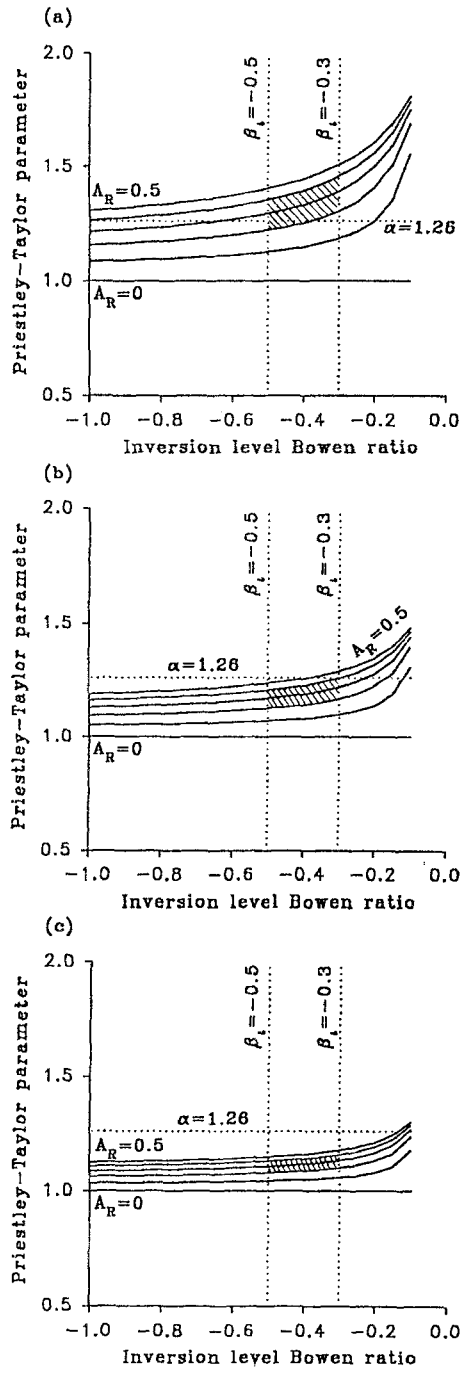

Fig. 5. Variation of the Priestley-Taylor parameter with the entrainment coefficient and the inversion-level Bowen ratio. (a) at 10 °C, (b) at 20 °C and (c) at 30 °C.

TABLE I

Values of α, α', β_s and β_s' calculated for typical values of β_i, A_R, c and T, where the primes denote values calculated using the simplified formulae (Equations 28 and 29).

T(°C)	A_R or c	β_i	β_s	α	β_s'	α'
10	0.2	−0.3	0.37	1.30	0.29	1.23
10	0.3	−0.3	0.28	1.39	0.26	1.30
10	0.4	−0.3	0.23	1.46	0.23	1.35
10	0.2	−0.5	0.47	1.22	0.31	1.18
10	0.3	−0.5	0.38	1.29	0.28	1.23
10	0.4	−0.5	0.32	1.35	0.26	1.29
20	0.2	−0.3	0.25	1.17	0.18	1.12
20	0.3	−0.3	0.19	1.22	0.17	1.16
20	0.4	−0.3	0.16	1.26	0.15	1.19
20	0.2	−0.5	0.29	1.13	0.19	1.09
20	0.3	−0.5	0.25	1.17	0.18	1.13
20	0.4	−0.5	0.21	1.20	0.16	1.16
30	0.2	−0.3	0.16	1.10	0.11	1.06
30	0.3	−0.3	0.13	1.13	0.11	1.09
30	0.4	−0.3	0.10	1.13	0.10	1.11
30	0.2	−0.5	0.18	1.08	0.12	1.05
30	0.3	−0.5	0.15	1.10	0.11	1.07
30	0.4	−0.5	0.13	1.16	0.10	1.09

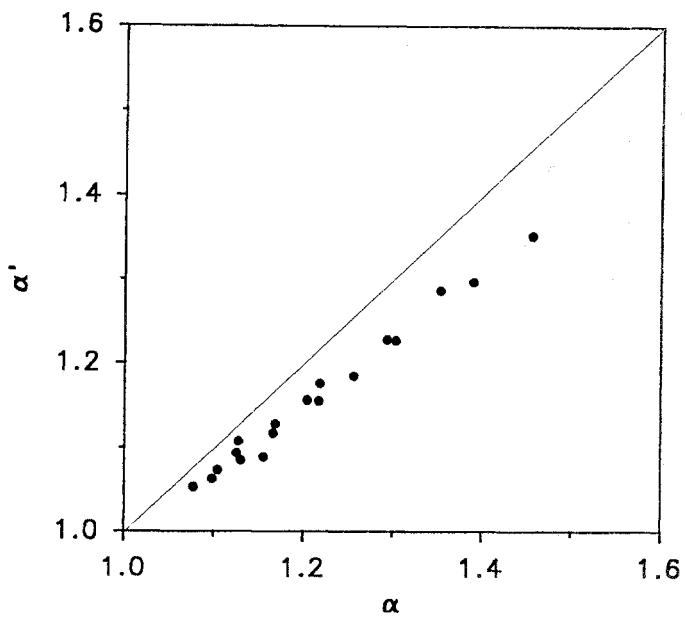

Fig. 6. The relationship between α calculated from Equation 24 and α' calculated from Equation 29.

that given by Equation (3). This difference is shown to be controlled by a complex function of A_R, β_i and ϵ and, consequently, even in ideal, advection-free (hypothetical?) conditions when evaporation might be expected to approach the equilibrium rate, the variability in these atmospheric parameters will lead to a range of values of α being observed.

Acknowledgements

The author acknowledges the financial support provided by the NERC through its TIGER (Terrestrial Initiative in Global Environment Research) programme, award number GST/91/III.1/1A.

References

Betts, A. K.: 1992, 'FIFE Atmospheric Boundary Layer Budget Methods', *J. Geophys. Res.* **97**, D17, 18,523–18,531.

De Bruin, H. A. R.: 1983, 'A Model for the Priestley-Taylor Parameter α', *J. Clim. Appl. Meteorol.* **22**, 572–580.

Culf, A. D.: 1992, 'An Application of Simple Models to Sahelian Convective Boundary Layer Growth', *Boundary-Layer Meteorol.* **58**, 1–18.

Driedonks, A. G. M.: 1981, 'Dynamics of the Well Mixed Atmospheric Boundary Layer', Scientific report W.R.81–2. pp. 189. K.N.M.I., de Bilt, The Netherlands.

McNaughton, K. G.: 1976, 'Evaporation and Advection I: Evaporation from Extensive Homogeneous Surfaces', *Quart. J. Roy. Meteorol. Soc.* **102**, 181–191.

McNaughton, K. G. and Jarvis, P. G.: 1983, 'Predicting Effects of Vegetation Changes on Transpiration and Evaporation', in T. T. Kozlowski (ed.), *Water Deficits and Plant Growth*, Vol. VII, pp. 1–47. Academic Press, New York.

McNaughton, K. G. and Spriggs, T. W.: 1986, 'A Mixed Layer Model for Regional Evaporation', *Boundary-Layer Meteorol.* **34**, 243–262.

Monteith, J. L., 1981, 'Evaporation and Surface Temperature', *Quart. J. Roy. Meteorol. Soc.* **107**, 1–27.

Pereira, A. R. and Villa Nova, N. A. 1992, 'Analysis of the Priestley-Taylor Parameter', *Agric. For. Meteorol.* **61**, 1–9.

Priestley, C. H. B. and Taylor, R. J.: 1972, 'On the Assessment of Surface Heat Flux and Evaporation', *Mon. Weath. Rev.* **106**, 81–92.

Shuttleworth, W. J. and Calder, I. R.: 1979, 'Has the Priestley-Taylor Equation any Relevance to Forest Evaporation?', *J. Appl. Meteorol.*, **18**, 638–646.